ASSESSING EXTRATERRESTRIAL REGOLITH MATERIAL SIMULANTS FOR IN SITU RESOURCE UTILISATION BASED 3D PRINTING

Athanasios Goulas[a], Jon G.P. Binner[b], Russell A. Harris[c], Ross J. Friel[a]

[a] *Wolfson School of Mechanical, Electrical & Manufacturing Engineering, Loughborough University, Loughborough, Leicestershire, LE11 3TU, United Kingdom*

[b] *College of Engineering and Physical Sciences, University of Birmingham, Edgbaston, Birmingham, B15 2TT, United Kingdom*

[c] *Mechanical Engineering, University of Leeds, Leeds, LS2 9JT, United Kingdom*

ABSTRACT

This research paper investigates the suitability of ceramic multicomponent materials, which are found on the Martian and Lunar surfaces, for 3D printing (aka Additive Manufacturing) of solid structures. 3D printing is a promising solution as part of the cutting edge field of future in-situ space manufacturing applications.

3D printing of physical assets from simulated Martian and Lunar regolith was successfully performed during this work by utilising laser-based powder bed fusion equipment. Extensive evaluation of the raw regolith simulants was conducted via Optical and Electron Microscopy (SEM), Visible-Near Infrared/Infrared (Vis-NIR/IR) Spectroscopy and thermal characterisation via Thermogravimetric Analysis (TGA) and Differential Scanning Calorimetry (DSC). The analysis results led to the characterisation of key properties of these multicomponent ceramic materials with regards to their processability via powder bed fusion 3D printing.

The Lunar and Martian simulant regolith analogues demonstrated spectral absorbance values of up to 92% within the Vis-NIR spectra. Thermal analysis demonstrated that these materials respond very differently to laser processing, with a high volatility (30% weight change) for the Martian analogue as opposed to its less volatile Lunar counterpart (<1% weight change). Results also showed a range of multiple thermal occurrences associated with melting, glass transition and crystallisation reactions. The morphological features of the powder particles are identified as contributing to densification limitations for powder bed fusion processing.

This investigation has shown that – provided that the simulants are good matches for the actual regoliths – the lunar material is a viable candidate material for powder bed fusion 3D printing, whereas Martian regolith is not.

KEYWORDS

3D printing; additive manufacturing; regolith; simulants; ISRU; space

1 Introduction

Human presence in Low Earth Orbit (LEO), a return to the Moon and both manned and unmanned missions to the planet Mars are the next human-centric goals set by the major space agencies [1,2]. Further exploration into the solar system and to nearby planetary bodies, or perhaps even the outer planets, could be made more viable by establishing Extra-Terrestrial (ET) bases which could serve as launch/landing pads or even mid-mission supply outposts [3]. The concept of on-site resource utilisation has been discussed in the literature with envisioned methods of building Lunar and Martian bases/structures being investigated [4–7]. Application areas for the intended builds include: infrastructure, shielding against meteoroids, solar and cosmic radiation and for building physical assets intended for part replacement purposes. 3D printing, also known as Additive Manufacturing (AM), is a group of advanced manufacturing technologies that offer automated production and that could potentially be achieved extra-terram. These technologies fabricate physical components directly from computer data and a wide range of materials (covering metals, ceramics, polymers and composites) using a layer-by-layer building strategy.

A prevailing concept is to ship 3D printing equipment to the prospective extra-terrestrial locations (i.e. the Moon, Mars etc.), that would function autonomously and utilise indigenous materials as feedstock [8–11]. Previous studies have demonstrated that the application of a Powder Bed Fusion 3D printing process can manufacture structures/components from multi-component ceramics that closely simulate Lunar and Martian regolith [12,13]. The need to use simulants is due to the scarcity of actual ET materials on Earth; there is a very small, closely guarded quantity of Lunar material and no samples acquired from Mars [14]. Although the concept of utilising the regolith materials to create 3D objects via 3D Printing has been proven,

the investigation and characterisation of these material's properties, and the mechanisms of the interaction with the 3D printing process, have so far not been performed.

The various planetary regolith simulants, that are available in the research community, have been developed over the last few decades by various countries and for numerous reasons. Although they are perceived as "effective copycats" they are clearly not actual Lunar and Martian materials. The original design of these simulants was the successful replication of basic engineering properties, such as particle size and shape distribution, and also composition of close matching chemistry and mineralogy, they have not been specifically developed in order to provide answers to more sophisticated technology and material processing investigations, such as the one of 3D printing. For the time being, it is not possible to have a single simulant material that will satisfy all scientific or engineering investigations [15]; therefore the choice of an appropriate simulant has to be conducted according to the pertinent material properties that would best match the intended application. It must be acknowledged that the scientific literature that has been put together from studying the lunar soil samples brought back to Earth and also the results from the in-situ analyses conducted on board both the Lunar and Martian landers have provided a wealth of information, however there is still a gap in the knowledge with regards to the material processing characteristics of the actual versus simulant materials.

The current work consists of an investigation into the properties of regolith materials – which act to simulate the engineering characteristics, bulk chemistry, mineralogy and related properties of Lunar and Martian soils – that are critical to successful processing via powder bed fusion based 3D printing.

The work combines a number of well-established experimental techniques in order to investigate the materials' performance, with respect to areas of key importance for powder bed fusion; viz. a) optical and thermal properties, b) material stability under intense thermal input and c) internal morphological features of the powder feedstock.

The investigation has been carried out using state-of the art material analogues that are available for study. Their usage was based on their close matching chemistry, mineralogy and particle makeup characteristics to the actual materials that have been found and analysed on the Moon and Mars.

The investigation results provide an in-depth understanding of how the inherent materials' properties are likely to impact on the processing success. These can be extrapolated to make an assessment on whether or not the laser based powder bed fusion techniques are a potentially viable solution for future in-situ planetary (i.e. on the Moon or Mars) manufacturing.

2 Experimental

2.1 Materials

The research was carried out using commercially available simulants, developed and supplied by Orbital Technologies Corporation, Colorado, USA in coordination with the Johnson Space Centre at NASA. The Lunar simulant JSC-1A has been characterized as a crushed basalt, rich in glass and oxidized forms of silicon, aluminium, iron, calcium and magnesium [6], with a composition matching actual lunar mare soil. The simulant was initially developed as a terra-mechanical analogue in order to investigate various (i.e. excavation, traction, material handling etc.) engineering efforts to support future human lunar activities and it is considered as the best available replica on Earth. It is a representative of the dark basaltic plains on the Lunar surface, since the whole Lunar surface does consist of the same material. The simulant contains less material complexities compared to actual Lunar regolith, due to not having been exposed to "space weathering" conditions such as solar and cosmic ionising radiation, micro-meteoroid bombardment, etc. [16].

The Martian simulant material JSC-MARS-1A consists mainly of palagonitic tephra (weathered volcanic ashes) and was mined on Earth in a cinder cone in Hawaii, USA. This material was chosen due to its spectral similarities to the regolith collected by the Viking landers, Mars and Spirit Rovers and analysed on board using Fluroscence (XRF) and Alpha Particle X-ray Spectrometry (APXS) [17–19]. It is as accurate a representation of the local regolith at the landing sites (once again, the material varies across the planet) that can be achieved until actual regolith is brought to Earth.

Both materials were stored and handled at all times, under controlled temperature and humidity laboratory conditions of 23 °C and 50% relative humidity (RH) and prior to any processing were preheated in a laboratory thermal oven for 1 hour at 300°C in order to remove any adsorbed humidity from the laboratory ambient air.

Table 1 shows the chemistry present in both simulants, as given by the materials' supplier datasheets, and a comparison from the real samples as acquired and analysed with a variety of observational data [20].

Table 1 *– Composition (Wt. %) of the major constituents in the JSC-1A Lunar Regolith Simulant and JSC-MARS-1A Martian Regolith Simulant.*

Chemical Compound	*Lunar Regolith Simulant (Orbitec, 2005).*	*Lunar Regolith - Actual (Sample 14163) (Morries et al. , 1983)*	*Martian Regolith Simulant (Orbitec, 2008).*	*Martian Regolith – Actual (Allen et al., 1998)*
Silicon dioxide (SiO_2)	46 - 49	47.3	34.5 – 44	43 – 44
Titanium dioxide (TiO_2)	1 - 2	1.6	3 – 4	0.56 – 1.1
Aluminium oxide (Al_2O_3)	14.5 – 15.5	15	18.5 – 23.5	7 – 7.5
Ferric oxide (Fe_2O_3)	3 - 4	3.4	9 – 12	16.5 – 18.5
Iron oxide (FeO)	7 – 7.5	7.4	2.5 – 3.5	N.D.
Magnesium Oxide (MgO)	8.5 – 9.5	9	2.5 – 3.5	6 – 7
Calcium oxide (CaO)	10 – 11	10.4	5 – 6	5.6 – 5.9
Sodium oxide (Na_2O)	2.5 – 3	2.7	2 – 2.5	2.1
Potassium oxide (K_2O)	0.75 – 0.85	0.8	0.5 – 0.6	0.15 – 0.3
Manganese oxide (MnO)	0.15 – 0.20	0.2	0.2 – 0.3	N.A.
Chromium III oxide (Cr_2O_3)	0.02 – 0.06	-	–	
Diphosphorus pentoxide (P_2O_5)	0.6 – 0.7	0.7	0.7 – 0.9	N.A.

2.2 Analytical Method

2.2.1 Spectrometry

The optical properties that are of interest are the absorbance *a (λ)*, transmittance *t (λ)* and reflectance *r (λ)*. All three parameters are wavelength dependent and are connected through the energy conservation theorem, where an emitted photon must either be reflected, absorbed or transmitted when it interacts with a surface. Absorbance is defined as the ratio of the absorbed radiation to the incident radiation and is dependent on a series of factors that are related to the:

- laser system's operating wavelength
- processing environment, including ambient gas and temperature
- properties of the material, visual, surface geometry, powder thermo-physical properties, powder bed surface roughness, particle re-arrangement, phase transitions, chemistry, oxidation reactions, etc. [21].

The spectral absorbance characteristics of the regolith simulants were investigated in two different wavelength bands, 0.4 – 1.1 μm and 8 – 14 μm, that include the operating wavelengths of major laser systems used in industry for processing similar materials and also exist in state-of-the-art laser additive manufacturing equipment to date. Visible (VIS) to Near infra-red (NIR) spectra were obtained using a UV/VIS spectrophotometer (Lambda Bio 40, Perkin-Elmer, Überlingen, Germany) fitted with a Labsphere RSA-PE-20 reflectance accessory and referenced with a barium sulphate ($BaSO_4$) powder sample. Infra-red (IR) spectra were obtained using an FTIR spectrophotometer (FTIR-8400Sk, Shimadzu, Kyoto, Japan). Measurements were taken at 23°C and 55% RH conditions, using regolith powder samples initially screened with a laboratory

test sieve (Retsch GmbH), equipped with 125 µm apertures. The resulting particle size distribution after sieving, that was used for this study, is shown in the following **Table 2**, as measured by laser diffraction (Mastersizer Sirocco 2000 particle size analyser, Malvern Instruments Ltd., UK); **Figure 1**.

Table 2 *– Particle size analysis of Lunar (JSC-1A) and Martian (JSC-MARS-1A) regolith simulants.*

Simulant	D(0.1) (µm)	D(0.5) (µm)	D(0.9) (µm)	D(3.2) (µm)	D(4.3) (µm)	Span	Uniformity
JSC-1A	24.88	75.85	149.98	42.78	82.75	1.68	0.51
JSC-MARS-1A	23.30	67.96	137.33	34.06	75.12	1.65	0.52

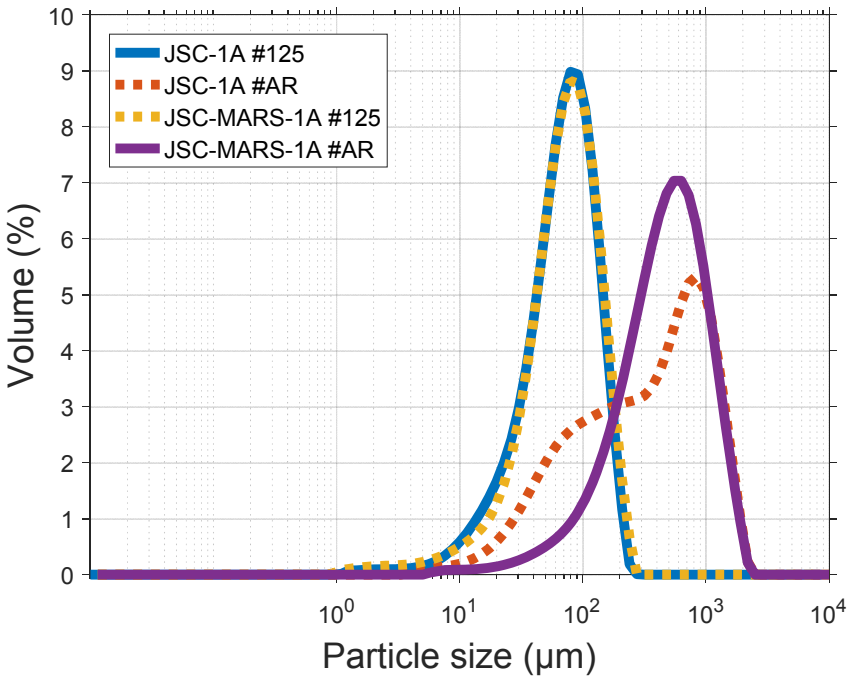

Figure 1 *– Particle size distribution comparison between the as received (#AR) and the sieved (#125) regolith simulant raw materials used in the study.*

2.2.2 Thermal Analyses

The stability of the regolith simulants during thermal processing was investigated by Thermo-Gravimetric Analysis TGA (Q5000-IR, TA Instruments Inc., USA), and Differential Scanning Calorimetry DSC (2920 Modulated DSC, TA Instruments Inc., USA). TGA was used to quantify the materials' mass loss whilst DSC was used to identify the range of melting temperatures and any thermo-physical material interactions during heating. Both techniques were operated under an argon gas environment with 200 ml min^{-1} purging rate, at a heating rate of 10°C min^{-1}, from room temperature up to 1000°C. All samples were introduced in high purity alumina crucibles with an empty pan used as a reference to calibrate the baselines.

2.2.3 Microscopy

Morphological features of the Lunar and Martian regolith simulants, including particle surfaces and internal porosity, was investigated by using optical (Eclipse MA200, Nikon Instruments Europe, Netherlands) and scanning electron microscopy SEM (TM 3030 SEM, Hitachi High-Technologies Europe GmbH, Germany). Both powder and fused samples (see section 3.3) were prepared for SEM via a standard metallography regime on an automated polishing machine (AutoMet 250, Buehler Inc., USA) mounted in epoxy resin (EpoThin2, Buehler Inc., USA) and ground using silicon carbide paper from P320 to P4000. After grinding, polishing was carried out using polishing cloths with 1 µm diamond and 0.05 µm alumina suspensions. Specimens were sputter coated for 60 seconds at 20 mA using a gold/palladium alloy in a 80:20 ratio.

The relative porosity of the fabricated samples and the feedstock materials particles were quantified using SEM imaging of cross-sections. The acquired images were processed and binarized using a suitable threshold value and the relative porosity was calculated as a ratio of the black to white pixels that corresponded with the fraction of the surface voids over the total surface [22]. The pore size distribution of the fabricated samples has been calculated from a minimum of 5 3D printed samples. For the feedstock materials' particles 30 SEM micrographs of mounted and prepared samples have been used and thoroughly assessed to depict the internal morphology of isolated particles.

2.3 3D Printing equipment

All additively manufactured test samples, **Figure 2**, used in this study, were built using a Selective Laser Melting (SLM) machine, (SLM100A, Realizer GmbH, Borchen, Germany). The SLM100A utilised an ytterbium-doped fibre laser, manufactured by IPG Photonics, Oxford, Massachusetts, USA, with a central emission wavelength of 1.06 μm and a standard TEM_{00} Gaussian profile beam with a maximum power output of 50 W. The 120 mm f-theta lens used by the machine was able to focus the beam down to 80 μm diameter. All manufactured samples were built on a cylindrical Ø120x10 mm EN 1.4841 / AISI 314 stainless steel substrate plates that were previously coated in regolith simulant and heated to a constant temperature of 200 ± 2°C to reduce the thermal gradient during processing.

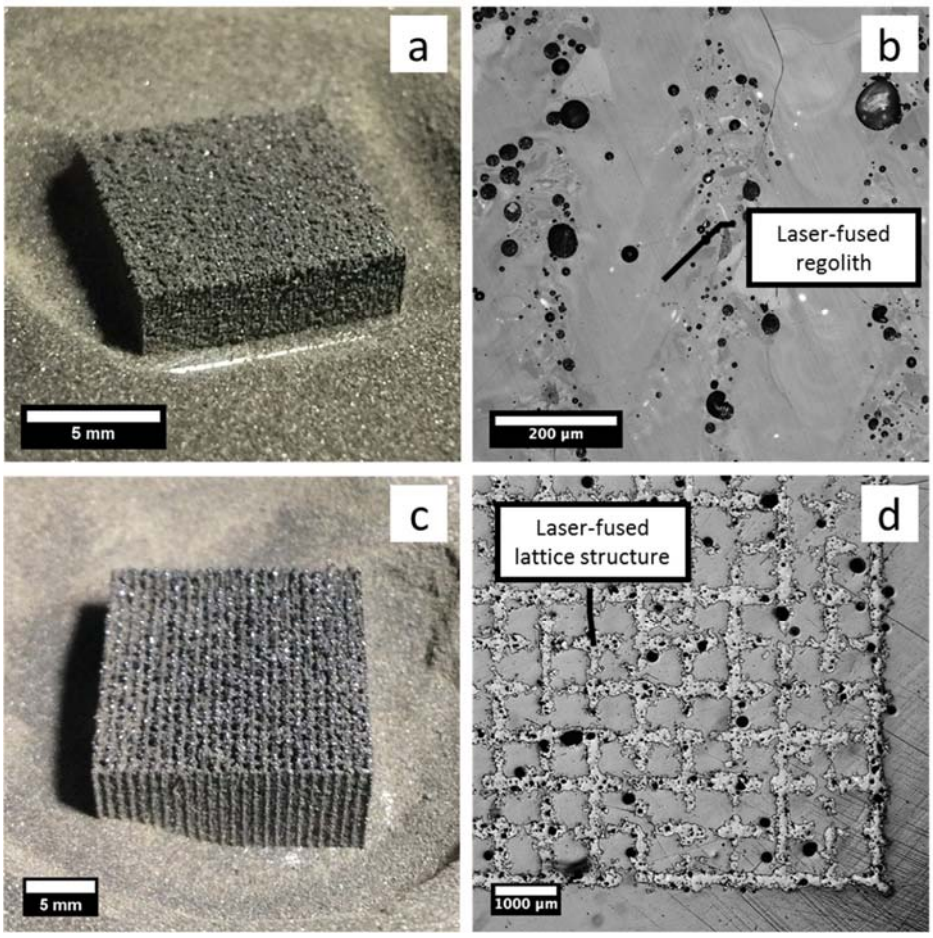

Figure 2 *– Examples of the 3D printed test pieces: (a) and (c) built from Lunar regolith simulants and their accompanying optical micrographs, (b) and (d), showing microscale features.*

3 Results and Discussion

3.1 Spectral Absorbance

In powder bed fusion, a proportion of the laser beam penetrates the surface material through porosity or intergranular voids that arise from the low packing density of the angular particles of the simulants. The laser thus interacts with both particles in the top layer and below it, leading to a degree of particle re-arrangement and hence changes in the absorbance characteristics of the material [23]. It should be noted that the absorbance values of a powder bed is much higher in comparison than for the equivalent solid material surface due to the air gaps acting as a black body and thus boosting light absorption [24].

The absorbance characteristics of the regolith simulants was the first parameter to be investigated, since it aided the development of an understanding of the nature of the interaction between the incident electromagnetic radiation and the material and thus assisted in determining the optimum irradiation wavelength for material fusion. It is self-evident that the greater the absorbance value of a material the less energy input is needed for it to be adequately fused. In addition, it is important to avoid excessive energy input since it can cause unwanted process-induced effects such as vaporization, irregularities, insufficient fusion, etc.

Figure 3 shows the absorbance values of the regolith simulants in (a) the visible/NIR and (b) the IR spectra. It was evident that that the materials had dissimilar characteristics which suggests that the prospective laser 3D printing equipment and power source, should be capable to work with a wide range of operating wavelengths in order to satisfy the processing requirements of various planetary regolith materials. Although expected, this is nonetheless a significant result,

in that potential manufacturing processes for autonomous planetary construction will have to be designed and built to suit a wide range of material properties in the intended construction locale.

In the IR spectrum both materials exhibited low absorption values, however the Martian simulant had a larger absorbance value (0.27) in comparison to that of the Lunar material (0.16). In the NIR spectrum, both materials exhibited good absorbance characteristics, where the Lunar material presented a value of up to 0.92 and the Martian material of up to 0.60.

The results acquired via spectrometry revealed that the ytterbium-doped fibre laser used in this study, which operated in the near infrared spectrum (λ = 1.06 μm), was a promising candidate system since it was better absorbed, in comparison to a commonly used CO_2 (λ = 10.6 μm) laser, by both materials and hence less energy input would be required in order to achieve fusion between the particles of the feedstock material.

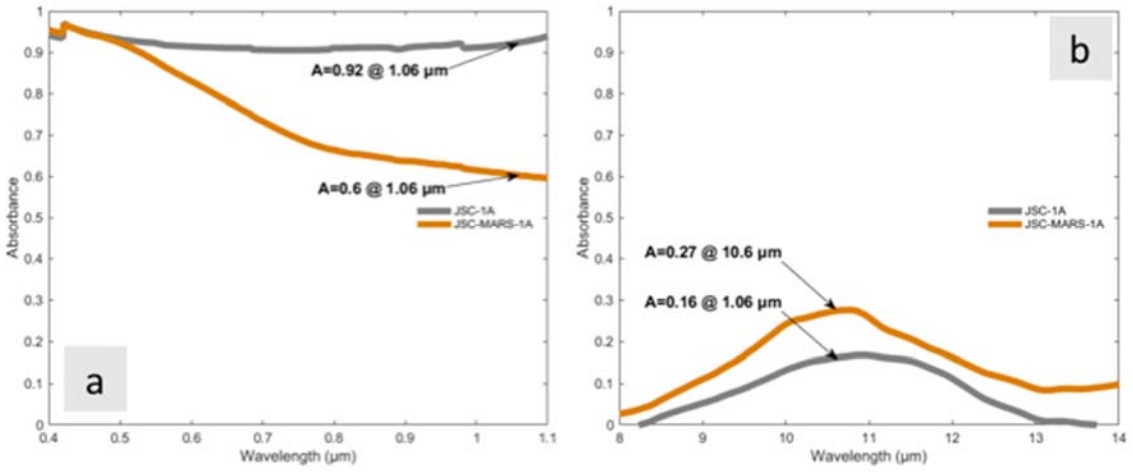

Figure 3 *– Absorbance of regolith simulants in (a) the visible to near infrared (Vis-NIR) spectra and (b) infrared (IR) spectra.*

3.2 Thermal Analysis

TGA data for the Lunar regolith simulant did not reveal weight changes beyond ±1%. A minimum weight loss of 0.03% was recorded at the temperature of 323°C suggesting the evaporation of H_2O molecules that had either adhered on the surface of the materials particles whilst exposed into the ambient laboratory air or were dehydrated from its microcrystalline secondary mineral constituents [25]. A small mass gain of 0.73% recorded at 659^{o}C was evident and is likely to have been due to oxidation reactions of the iron oxide compounds present [26]. Respective TGA data for the Martian counterpart material revealed a continuous trend of decomposition and mass loss up to 30% from room temperature up to the highest recorded temperature of 963°C.

This significant mass loss is explainable by dehydration reactions and also the presence of magmatic carbonate and sulphur dioxide [27]. The volcanic ores used as the Martian simulant material are known to contain water molecules (the result of volcanic ash weathering) that are retained up to very high temperatures and both crystalline and amorphous carbonate content that usually outgasses at elevated temperatures. Given the recent confirmed evidence regarding traces of water identified on Mars [28], it is suggested that any aqueous content is likely to affect the performance of the actual Martian regolith in a similar manner.

An overlay of the TGA curves of both materials is shown in **Figure 4** and clearly shows the volatile behaviour of the Martian regolith simulant as opposed to the thermally stable Lunar material. The fact that the material evaporated across a range of laser density inputs anticipated poor laser fusion behaviour, a result that was verified during the laser processing of the material. This high

volatility of the Martian regolith simulant resulted in builds with poor inter-laminar and lateral consolidation of the particles and intense porosity; **Figure 5**.

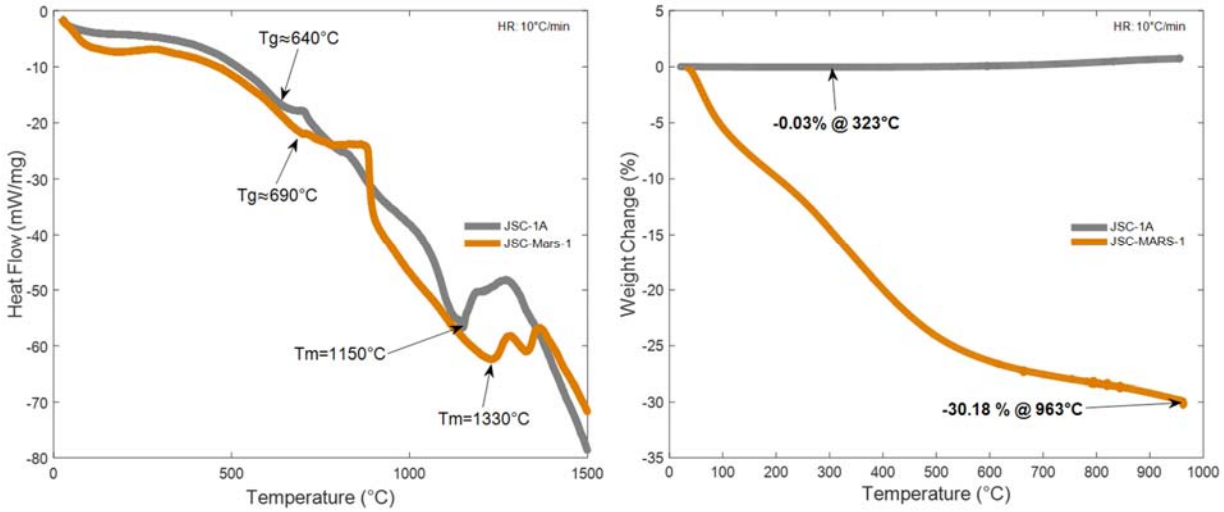

Figure 4 *– DSC (left) & TGA (right) curves overlay of Lunar and Martian Regolith Materials.*

After optical analysis, the thermal behaviour of a material is the second major factor that needs to be taken into account for powder bed fusion and is of utmost importance due to the fundamental requirement of the material to be stable under a range of thermal loads induced during laser irradiation. The present work confirms the necessity of investigating the presence of any volatile components in the candidate regoliths body as part of the assessment of suitability for thermal-based laser 3D printing.

Calorimetric data was also successfully acquired for both materials, in order to identify the melting behaviour and complete the thermal profile of the regolith simulants. Results in both cases depicted a plethora of exo and endo-thermal events associated with phenomena such as glass transition, crystallisation, phase transformation and finally melting events for the multiple

crystalline phases present in the materials. The Lunar material showed a basaltic glass transition at 640°C and a major endothermic peak at 1150°C, which is associated with its melting temperature. The Martian material showed a glass transition temperature at 690°C together with multiple endothermic peaks, suggesting melting at a maximum temperature of 1330°C. The melting temperature in regoliths is mainly dependent on the chemistry and abundance of glass content [25] and is important to identify in order to calculate the required amount of heat input for efficient and adequate melting of the feedstock. From an application point of view this result is also important in order to predict the built assets' ability to withstand thermal loads, e.g. for re-entry shielding [29].

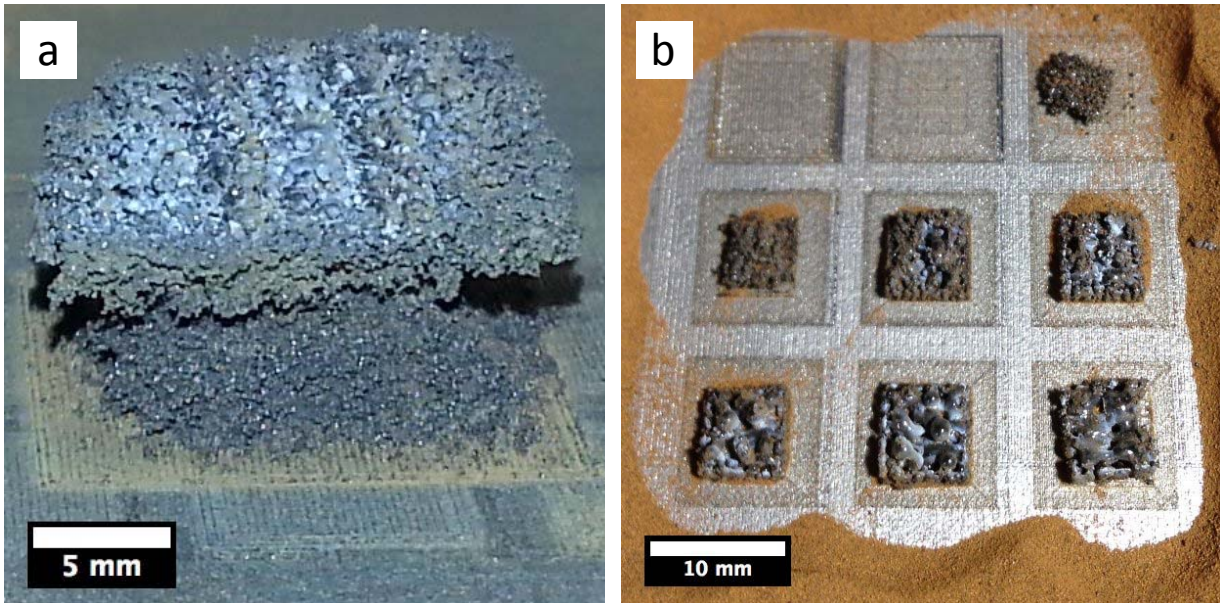

Figure 5 *– Examples of build samples using the JSC-MARS-1A regolith simulant, with poor inter-laminar (a) and planar (b) consolidation as a result of thermal instability (volatile behaviour of material).*

3.3 Microscopy Analysis

Examples of pre-processed material particle internal porosities are shown through SEM image cross-sections in **Figure 6**. Measurements identified a 7.72 ± 0.3% pre-processing porosity for the Lunar simulant, whereas the Martian simulant exhibited a higher value of 24.3 ± 7.2%. In the following graph; **Figure 7**, the porosity pre and post laser processing is presented. For the Lunar and Martian post laser processed samples the porosity values were reduced to 4.3 ± 0.5% and 21 ± 3% respectively. The percentile reduction in porosity as a result of consolidation and unification of the particles, due to laser processing, was 43.8% for the Lunar regolith and 13.6 % for the Martian. Apart from the complex angular and irregular morphology of the feedstock granular material, which resulted in bed performance deficiencies such as reduced followability [30], sub-optimal packing density, inter-particle friction [31] etc., it has been identified that the highly porous nature of the pre-processed Martian regolith is another important factor, affecting the potential of the material to be effectively fused via laser.

Packing density is a common challenge in powder bed fusion, where successful interlaminar consolidation in layered manufacturing relies upon effective consecutive deposition of fine powder layers of the material. Besides morphology issues mentioned above, the internal porosity which was inherent from the regolith's igneous and mineral origin, led to the formation of inter-particle voids. As well as dispersing the laser irradiation, these voids will entrap small quantities of gas during deposition of the next layer of powder. These then outgas during processing preventing the molten material from infiltrating, via capillary forces, any voids formed between adjacent powder layers [32].

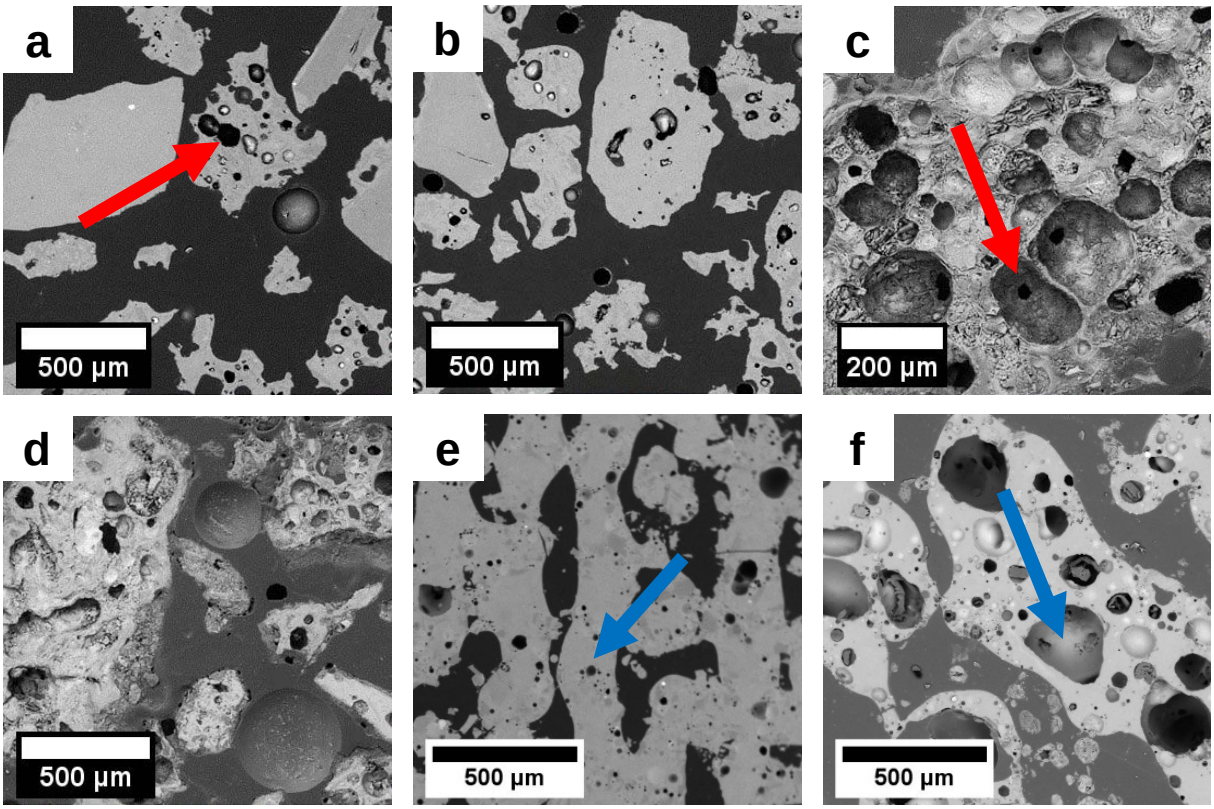

Figure 6 *– SEM images of pre-processed regolith cross-sections; Lunar (a, b) and Martian (d, e). Images c (Lunar) and f (Martian) show the laser fused samples. The red arrow denotes the internal porosity of granular material suggested to be contributing to the build parts' formed porosity, as shown with the blue arrows.*

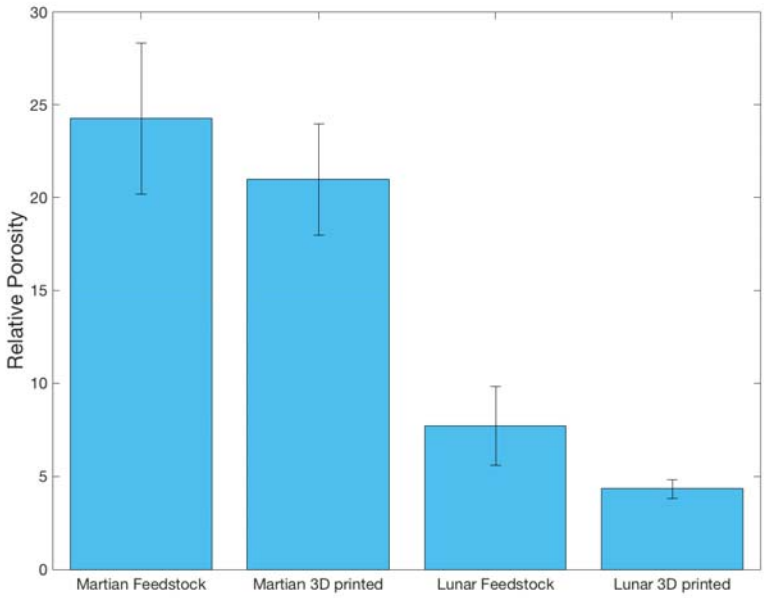

Figure 7 *– Relative porosity (%) comparison pre (feedstock) and post (3D printed) laser processing between the Lunar (JSC-1A) and Martian (JSC-MARS-1) regolith material.*

4 Conclusions

This study has documented an experimental investigation into the optical and thermal properties, as well as the morphology, of two different ceramic multi-component regoliths that match the engineering properties, bulk chemistry and mineralogy of Lunar soil and Martian soil. Although the regolith simulants used in this study were based on actual extra-terrestrial soil samples collected/analysed in-situ, the respective original samples were collected from a single area and thus they are expected to vary across both planetary bodies. The data collected in this study has shed insight into the understanding of these materials' inherent properties and how they affect the utilisation of the material for powder bed fusion-based 3D printing. However, the issues of reduced gravity and its impacts on processing have not been taken into account in this study and they would be important to research prior to any actual construction mission to the Moon or Mars.

Spectral absorbance measurements have shown favourable behaviour for both the Lunar and Martian materials in the visible to near-infrared band (0.4 – 1.1 μm) with absorbance values of up to 92% for the Lunar regolith and 60% for its Martian counterpart, as opposed to their high reflective performance on the far infrared band (8 – 14 μm) with absorption values as low as 16% and 27% respectively. This suits current powder bed fusion systems' thermal energy sources since they typically fall within the range of 0.4 – 1.1 μm.

Results from the thermal analysis have shown the significantly volatility of the Martian simulant, with a recorded weight loss of up to 30% as compared to <1% weight loss of its Lunar comparator. This result demonstrates that the Martian regolith is less likely to be able pose as a viable

feedstock for thermal based processing such as powder bed fusion. This means that powder bed fusion 3D printing systems could be suitable for Martian manufacturing and that careful identification and analysis of extra-terrestrial materials would be vital prior to any future planned exploration.

Further analysis of the acquired thermal profiles for both materials have shown a maximum melting temperature of 1150°C for the Lunar regolith and 1330°C for the Martian material; in addition, there are a plethora of thermal events up to 1500°C associated with thermo-physical reactions of melting and crystallisation of their multicomponent constituents. These results clearly indicated the challenging nature of these materials and have helped identify the requirements for tailoring processing strategies if successful fusion is to be achieved.

The angular and irregular morphology of the simulant particles are believed to account for the poor packing performance of the regolith into the powder bed. In addition, the internal porous nature of the Martian simulant, with a porosity value of 24.3% when compared to the Lunar one of 7.73%, has been identified as a contributing factor to the inability to achieve an optimum densification after laser fusing the granular material.

The understanding of the materials' intrinsic characteristics, combined with thermal energy source knowledge, allows the engineering of an optimal set of manufacturing parameters for in-situ building of components and physical assets out of Lunar/Martian extra-terrestrial materials for planetary applications.

Future work in this specific area will include further investigation of processing solutions tailored to the specific materials' properties that could tackle the poor densification results encountered

during powder bed fusion processing. These include: alternative thermal input systems that operate at wavelengths that are more absorbed, changing of processing atmosphere to better simulate off-word conditions (i.e. vacuum); and artificially altering the percentage of constituting elements via the introduction of dopants, to achieve enhanced densification.

Acknowledgments

The authors would like to thank the experimental officers in Loughborough Materials Characterisation Center (LMCC) for their assistance.

5 References

[1] B. Hufenbach, T. Reiter, E. Sourgens, ESA strategic planning for space exploration, Space Policy. 30 (2014) 174–177. doi:10.1016/j.spacepol.2014.07.009.

[2] T.P. Gouache, N. Patel, C. Brunskill, G.P. Scott, C.M. Saaj, M. Matthews, L. Cui, Soil simulant sourcing for the ExoMars rover testbed, Planet. Space Sci. 59 (2011) 779–787. doi:10.1016/j.pss.2011.03.006.

[3] J.A. Happel, Indigenous Materials for Lunar Construction, Appl. Mech. Rev. 46 (1993) 313. doi:10.1115/1.3120360.

[4] W.Z. Sadeh, M.E. Criswell, Infrastructure for a Lunar base, Adv. Sp. Res. 18 (1996) 139–148.

[5] S. Sen, C.S. Ray, R.G. Reddy, Processing of lunar soil simulant for space exploration applications, Mater. Sci. Eng. A. 413–414 (2005) 592–597.

[6] H. Arslan, S. Sture, S. Batiste, Experimental simulation of tensile behavior of lunar soil simulant JSC-1, Mater. Sci. Eng. A. 478 (2008) 201–207. doi:10.1016/j.msea.2007.05.113.

[7] H. Benaroya, L. Bernold, Engineering of lunar bases, Acta Astronaut. 62 (2008) 277–299. doi:10.1016/j.actaastro.2007.05.001.

[8] F. Ceccanti, E. Dini, X. De Kestelier, V. Colla, L. Pambaguian, 3D printing technology for a moon outpost exploiting lunar soil, in: 61st Int. Astronaut. Congr. Prague, CZ, IAC-10-D3, 2010: pp. 1–9. http://www.spacerenaissance.org/projects/LHD/Praga_Conference_Luna.pdf (accessed September 4, 2014).

[9] V.K. Balla, L.B. Roberson, G.W.O. OConnor, S. Trigwell, S. Bose, A. Bandyopadhyay, First Demonstration on Direct Laser Fabrication of Lunar Regolith Parts, Rapid Prototyp. J. 18 (2010) 451–457. doi:10.1108/13552541211271992.

[10] B. Khoshnevis, M. Bodiford, Lunar contour crafting—a novel technique for ISRU-based habitat development, in: 43rd AIAA Aerosp. …, 2005: pp. 1–12. http://arc.aiaa.org/doi/pdf/10.2514/6.2005-538 (accessed September 4, 2014).

[11] M. Fateri, K. Maziar, On-site Additive Manufacturing by Selective Laser Melting of composite objects, Concepts Approaches Mars Explor. 305 (2012) 842–845. doi:10.1126/science.3050842.

[12] A. Goulas, R.J. Friel, 3D printing with moondust, Rapid Prototyp. J. 22 (2016). doi:10.1108/RPJ-02-2015-0022.

[13] A. Goulas, R.A. Harris, R.J. Friel, Additive manufacturing of physical assets by using ceramic multicomponent extra-terrestrial materials, Addit. Manuf. 10 (2016) 36–42. doi:10.1016/j.addma.2016.02.002.

[14] H.A. Oravec, X. Zeng, V.M. Asnani, Design and characterization of GRC-1: A soil for lunar terramechanics testing in Earth-ambient conditions, J. Terramechanics. 47 (2010) 361–377. doi:10.1016/j.jterra.2010.04.006.

[15] L.A. Taylor, C.M. Pieters, D. Britt, Evaluations of lunar regolith simulants, Planet. Space Sci. (2016) 1–7. doi:10.1016/j.pss.2016.04.005.

[16] E.L. Patrick, K.E. Mandt, S.M. Escobedo, G.S. Winters, J.N. Mitchell, B.D. Teolis, A qualitative study of the retention and release of volatile gases in JSC-1A lunar soil simulant at room temperature under ultrahigh vacuum (UHV) conditions, Icarus. 255 (2015) 30–43. doi:10.1016/j.icarus.2015.03.015.

[17] C.C. Allen, R. V. Morris, M.J. Karen, D.C. Golden, M.M. Lindstrom, J.P. Lockwood, Martian Regolith Simulant JSC-Mars-1, in: Lunar Planet. Sci. Conf. XXIX, 1998: p. 1690.

[18] C.C. Allen, K.M. Jager, R. V. Morris, D.J. Lindstrom, M.M. Lindstrom, J.P. Lockwood, Martian soil stimulant available for scientific, educational study, Eos, Trans. Am. Geophys. Union. 79 (1998) 405–405. doi:10.1029/98EO00309.

[19] B. Bonin, Extra-terrestrial igneous granites and related rocks: A review of their occurrence and petrogenesis, Lithos. 153 (2012) 3–24. doi:10.1016/j.lithos.2012.04.007.

[20] T.L. Roush, Infrared optical properties of Mars soil analog materials: Palagonites, Lunar Planet. Inst. (1993) 32–33. http://adsabs.harvard.edu/abs/1993chwe.work...32R.

[21] N.K. Tolochko, Y. V. Khlopkov, S.E. Mozzharov, M.B. Ignatiev, T. Laoui, V.I. Titov, Absorptance of powder materials suitable for laser sintering, Rapid Prototyp. J. 6 (2000) 155–161. doi:10.1108/13552540010337029.

[22] K. Monroy, J. Delgado, J. Ciurana, Study of the pore formation on CoCrMo alloys by selective laser melting manufacturing process, Procedia Eng. 63 (2013) 361–369. doi:10.1016/j.proeng.2013.08.227.

[23] J.R. Gaier, S. Ellis, N. Hanks, Thermal Optical Properties of Lunar Dust Simulants and Their Constituents, J. Thermophys. Heat Transf. 26 (2011) 573–580. doi:10.2514/1.T3838.

[24] N. Hopkinson, R. Hague, P. Dickens, Rapid Manufacturing: An Industrial Revolution for the Digital Age, 2005. doi:ISBN: 978-0-470-01613-8.

[25] K.W. Street, Jr., C. Ray, D. Rickman, D. a. Scheiman, Thermal Properties of Lunar Regolith Simulants, Earth Sp. 2010. (2010) 266–275. doi:10.1061/41096(366)28.

[26] C.S. Ray, S.T. Reis, S. Sen, J.S. O'Dell, JSC-1A lunar soil simulant: Characterization, glass formation, and selected glass properties, in: J. Non. Cryst. Solids, Elsevier B.V., 2010: pp. 2369–2374. doi:10.1016/j.jnoncrysol.2010.04.049.

[27] C.C. Allen, R. V. Morris, M.J. Karen, D.C. Golden, M.M. Lindstrom, J.P. Lockwood, MARTIAN REGOLITH SIMULANT JSC MARS-1, in: Lunar Planet. Sci. Conf. XXIX, 1998: p. 1690.

[28] L. Ojha, M.B. Wilhelm, S.L. Murchie, A.S. Mcewen, J.J. Wray, J. Hanley, M. Massé, M.

Chojnacki, Spectral evidence for hydrated salts in recurring slope lineae on Mars, Nat. Geosci. (2015) 1–5. doi:10.1038/NGEO2546.

[29] M.D. Hogue, R.P. Mueller, L. Sibille, P.E. Hintze, D.J. Rasky, Extraterrestrial Regolith Derived Atmospheric Entry Heat Shields, in: U.S. American Society of Civil Engineers; New York, NY (Ed.), 2016 ASCE Earth Sp. Conf., Orlando, FL; United States, 2016: pp. 1689–1699.

[30] G. Lumay, F. Boschini, K. Traina, S. Bontempi, J.C. Remy, R. Cloots, N. Vandewalle, Measuring the flowing properties of powders and grains, Powder Technol. 224 (2012) 19–27. doi:10.1016/j.powtec.2012.02.015.

[31] E.O. Olakanmi, K.W. Dalgarno, R.F. Cochrane, Laser sintering of blended Al-Si powders, Rapid Prototyp. J. 18 (2012) 109–119. doi:10.1108/13552541211212096.

[32] J.P. Kruth, X. Wang, T. Laoui, L. Froyen, Lasers and materials in selective laser sintering, Assem. Autom. 23 (2003) 357–371. doi:10.1108/01445150310698652.